Quaternary Research (2017), **87**, 82–95.

doi:10.1017/qua.2016.6

Micromorphology of late Pleistocene and Holocene sediments and a new interpretation of the Holocene chronology at Anderson Pond, Tennessee, USA

Steven G. Driese[a,*], Sally P. Horn[b], Joanne P. Ballard[b], Mathew S. Boehm[b], Zhenghua Li[c]

[a]Terrestrial Paleoclimatology Research Group, Department of Geology, Baylor University, One Bear Place #97354, Waco, TX 76798-7354, United States
[b]Department of Geography, The University of Tennessee, 1000 Phillip Fulmer Way, Knoxville, TN 37996-0925, United States
[c]Earth and Environmental Sciences Division, Los Alamos National Laboratory, P.O. Box 1663, MS J535, Los Alamos, NM 87545, United States

(Received June 4, 2016; Accepted October 27, 2016)

Abstract

Thin-section (micromorphological) analysis of samples from the upper 1.5 m of a core obtained in 2007 from Anderson Pond, Tennessee, reveals a coherent but discontinuous record of late Pleistocene and Holocene climate change that supports some interpretations from previous pollen and charcoal analyses but indicates a revised Holocene chronology for this classic pollen site. Legacy sediments recording anthropogenic disturbance compose the upper 65 cm of the core (<160 cal yr BP) and are characterized by mixed, darker-colored, and coarser-grained deposits containing reworked soil aggregates, which sharply overlie finer-grained and lighter-colored, rooted middle Holocene sediments interpreted as a paleosol. These mid-Holocene sediments (95–65 cm; 7100–5600 cal yr BP) record extensive warm-dry subaerial soil conditions during the middle Holocene thermal maximum, manifested by illuviated clay lining root pores, and also contain abundant charcoal. Late Pleistocene sediments (150–95 cm), dark-colored and organic-rich, record open-water conditions and include siliceous aggregate grains at 143–116 cm (14,300–13,900 cal yr BP), recording intense fires. Thin sections are not commonly used in studies of paleoclimate from Quaternary lacustrine sediments, but we advocate for their inclusion in multianalytical approaches because they enhance resolution of depositional and pedogenic processes.

Keywords: Micromorphology; Pleistocene–Holocene; Paleoenvironment; Anderson Pond; Eastern Tennessee

INTRODUCTION

Micromorphology is the microscopic study of soils and sediments using thin sections. It is widely used in analysis of soils and paleosols to infer pedogenic processes and soil properties (Driese et al., 2007, 2016a, 2016b; Driese and Ashley, 2016) and to understand the architecture of processes of formation of unconsolidated glacial, periglacial, and marine sediments (van der Meer and Menzies, 2011). The technique is also important in the study of varved lake sediments (Clark, 1988; Brauer, 2004), for determining whether laminations are produced annually and for using the varved records and proxies within them to develop high-resolution records of climate, fire, and terrestrial and aquatic vegetation and biota. However, within the broader scope of Quaternary paleolimnological studies, the use of micromorphology is uncommon. This is unfortunate because much valuable paleoenvironment context can be secured using thin-section study, and the sediments themselves can be more fully characterized regarding textures and compositions. Our goal is to demonstrate the usefulness of thin-section micromorphology for reconstruction of late Quaternary paleoenvironments through application to Anderson Pond in eastern Tennessee. First cored by Delcourt (1979), who developed a pollen record that reached back to the last glacial period, the late Quaternary paleoecology of Anderson Pond has been studied and discussed by multiple researchers over the past four decades. The site has more than 5 m of Pleistocene lacustrine sediments but only a shallow (~1 m) Holocene record. Delcourt (1979) interpreted the upper part of the Anderson Pond record as demonstrating slow but continuous sedimentation across the Holocene, but Liu et al. (2013) suggested that much of the Holocene may be missing or disturbed, owing to erosional hiatuses and to bioturbation and mixing.

*Corresponding author at: Terrestrial Paleoclimatology Research Group, Department of Geology, Baylor University, One Bear Place #97354, Waco, TX 76798-7354, United States. E-mail address: Steven_Driese@baylor.edu (S.G. Driese).

OBJECTIVES

Using thin-section micromorphology, the objectives of this study are to examine the upper 1.5 m of a 2 m core obtained from Anderson Pond in 2007 (AP 2007-2, a core parallel to and presumably correlative with the longer AP 2007-1 core studied by Liu et al. [2013] recovered at the same time) for the following:

1. Evidence of major hiatuses or breaks in the sedimentation record.
2. Evidence for development of features indicative of drier climate during the middle Holocene thermal maximum (8000–4200 cal yr BP), previously suggested from pollen and microscopic charcoal analyses (Delcourt, 1979; Ballard et al., 2016), with evidence to be integrated with existing floodplain (Driese et al., 2008; Kocis, 2011) and speleothem (Driese et al., 2016a) paleoclimate records for the eastern Tennessee region.
3. Evidence for bioturbation. Previously, the upper 1.1 m interval of the Anderson Pond core AP 2007-1 was judged as unreliable and not datable by Liu et al. (2013) because of apparent sediment mixing and out-of-sequence radiocarbon dates. Thus, an important objective is to determine if there are bioturbation features that could have mixed younger charcoal and other macrofossils into deeper (and older) contexts or brought older material to the surface.
4. Occurrences of newly recognized sediment grain types that occur within a relatively narrow time interval of the late Pleistocene in the southeastern United States, which were termed "siliceous aggregate" grains by Ballard (2015) and Driese et al. (2015).

BACKGROUND

Geological and geomorphological setting

Anderson Pond is located on the eastern Highland Rim in east Tennessee (Fig. 1) and is developed in a sinkhole collapse formed within Mississippian-age marine carbonate (dolostone) deposits (Delcourt, 1978, 1979). It is located about 400–500 km south of the southernmost extent of the Laurentide Ice Sheet during the last glacial maximum (LGM) within an area of the southeastern United States that was not subjected to Pleistocene glaciation (Fig. 1). The Anderson Pond 1976 core sampled by Hazel and Paul Delcourt was interpreted as a largely continuous record of late Pleistocene (25,000 ^{14}C yr BP) to Holocene (and modern) deposition (Delcourt, 1978, 1979; Delcourt and Delcourt, 1980). Although Anderson Pond had 18 cm of water when sampled in 1976 by Delcourt (1979), she noted that water levels fluctuate 2–3 m throughout the year, with the basin supporting a large, deep pond in the winter but becoming a swamp with shallow, open pools when water levels are lowest in early autumn. Thickets of shrubs and small trees with interspersed marshes occupy the central portion of the sinkhole depression, surrounded by a ring of swamp forest with larger hardwoods

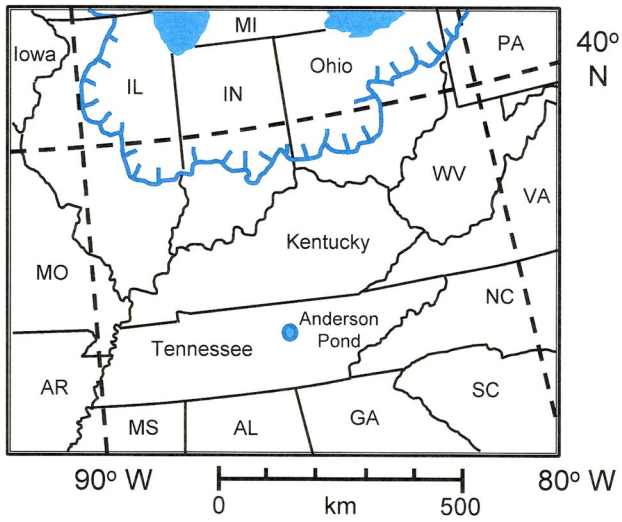

Figure 1. (color online) Map showing location of study site at Anderson Pond, on the eastern Highland Rim in Tennessee, USA. Note position of site relative to southernmost extent of Laurentide Ice Sheet (line, with tooth pattern) during the last glacial maximum (modified from Liu et al., 2013).

(Liu et al., 2013) that may be encroaching from the edges. There is no apparent stream that provides inflow or outflow, and the pond is spring fed (Delcourt, 1979). Water was low when we visited in June 2010 (Fig. 2), and there was no standing water at all during a prolonged drought in October 2007, when a team led by Stephen Jackson recovered the 7 m long AP 2007-1 core studied by Liu et al. (2013) and the parallel 2 m core that we studied, from a position (36°1'45"N, 85°30'4"W; 303 m elevation) estimated to be within 25 m of the original Delcourt (1979) sampling site (Liu et al., 2013).

Pollen records

The pollen record for Anderson Pond presented by Delcourt (1979) shows a dominance of boreal forest conifers (spruce

Figure 2. (color online) Field photograph of Anderson Pond site taken in June 2010 showing low water near the edge of the swamp and extensive hardwood vegetation.

https://doi.org/10.1017/qua.2016.6 Published online by Cambridge University Press

[*Picea*], jack pine [*Pinus banksiana*], and fir [*Abies*]) during the LGM, followed by a precipitous decline in these taxa and increase in oak and other deciduous forest taxa with late-glacial warming. From the pollen assemblages and from generally poor pollen and macrofossil preservation, she inferred warm and dry conditions during the middle Holocene at Anderson Pond. New pollen analyses presented by Liu et al. (2013) on the AP 2007-1 core largely reinforced the previous pollen work by Delcourt (1979) (for comparison diagram, see Ballard et al., 2016), but with the chronology improved by accelerator mass spectrometry (AMS) radiocarbon dating of macrofossils and constrained incremental sum of squares analysis used to guide delineation of pollen zones. In the upper 2 m that overlap with the parallel core we investigated, Liu et al. (2013) defined zone AP-3 (238–106 cm depth; 15.9–13.7 ka) as characterized by a dramatic decline in *Pinus*, with a steady rise in *Quercus* and *Ostrya*, along with low percentages of other deciduous forest taxa (*Acer*, *Carya*, *Fraxinus*, and *Ulmus*) and of grasses and sedges. Their zone AP-4 (106–0 cm depth; undated Holocene), in contrast, is characterized by high *Quercus* (30%–60%), *Carya* (10%–25%), and Poaceae (5%–15%); moderate *Pinus* (5%–20%); and low *Picea* and *Abies*. Liu et al. (2013) also noted a sharp increase in *Ambrosia* pollen above 35 cm, from about 1% to >20%, a spike they interpreted, as did Delcourt (1979), to be a consequence of Euro-American land clearance.

Sedimentary charcoal

Ballard et al. (2016) analyzed microscopic charcoal concentrations in Anderson Pond sediments and also calculated charcoal-to-pollen ratios, using the original pollen slides prepared by Delcourt (1978, 1979). They were unable to do additional dating on the 1976 core (of which only portions remain) but updated the original chronology by calibrating the radiocarbon dates reported by Delcourt (1979) using CALIB 7.0.2 and the IntCal13 database (Stuiver and Reimer, 1993; Reimer et al., 2013). Because their focus was to examine linkages between fire activity and the vegetation reconstruction developed by Delcourt (1979), they followed her approach of linear age modeling and assumption of continuous sedimentation, while acknowledging the possibility of a hiatus in the postglacial section of the 1976 record (Ballard et al., 2016). Comparing the ages of transitions in pollen assemblages identified by Liu et al. (2013) in their better-dated pollen record from the 2007 core with those evident in the Delcourt (1979) pollen record indicated an inconsistent offset for the glacial and late-glacial sediments, with a transition at 13,700 cal yr BP occurring some 900 yr later (12,800 cal yr BP) in the 1976 profile, but with three prior transitions occurring 500 to 2600 yr earlier (Ballard et al., 2016).

From the charcoal analysis, Ballard et al. (2016) determined the following: (1) fire activity was high from the LGM to ca. 15,000 cal yr BP, when spruce and pine pollen were abundant and jack pine was the dominant species (charcoal-to-pollen ratios are highest during this time); (2) fire activity was sharply reduced at ca. 15,000 cal yr BP, as conifers were replaced by hardwoods at the site, and remained low from ca. 15,000 to 8200 cal yr BP when fire-intolerant taxa such as *Ostrya* and *Carpinus* were important in the pollen record; (3) highest fire activity as indicated by charcoal area concentrations occurred during the middle Holocene thermal maximum (8200 to 5000 cal yr BP), coincident with increased percentages of indeterminate pollen grains interpreted to indicate poor preservation under drier conditions; and (4) charcoal area concentrations declined from 5000 cal yr BP to the present. However, it should be noted that Ballard et al.'s (2016) interpretations were based on an assumption of fairly continuous sedimentation and did not include the revised age-depth model with unconformities that we present in this study.

Previous age-depth models

The original age-depth model for Anderson Pond developed by Delcourt (1979) was based on conventional radiocarbon dates on bulk sediments with high uncertainties and likely some influence of an old carbon effect. These dates indicate that the sinkhole pond began filling with sediments at ca. 25,000 ^{14}C yr BP (Fig. 3), at least in chutes in the limestone bedrock, the depositional setting of the lowest ~2 m of the 1976 Anderson Pond record (Delcourt, 1979). Anderson Pond initially filled with mineral-rich sediments fairly rapidly (average sedimentation rate of 0.06 cm/yr), but the dates indicated an apparently sharp decline in sedimentation coincident with the deposition of more organic-rich sediments at ca. 12,750 ^{14}C yr BP, with the upper 1 m of sediments representing ca. 10,000 ^{14}C yr of deposition. A modern date (-10 ± 100 ^{14}C yr BP) was obtained on bulk sediment from 34 to 40 cm below the mud–water interface.

AMS dating of macrofossils in the new AP 2007-1 core by Liu et al. (2013) showed a modern date (115 ± 35 ^{14}C yr BP) at 67 cm depth (*Scirpus* and Polygonaceae seeds) and a date of less than modern at 86 cm (Polygonaceae seeds and twig) that was regarded as erroneous and discarded. Based on the AMS dates and the results of Bayesian age modeling with the Bacon program (Blaauw and Christen, 2011), which together suggested a hiatus and sediment mixing in the upper meter, Liu et al. (2013) concluded that the sediment stratigraphy and chronology of their Anderson Pond core was unreliable above 106 cm (<13,700 cal yr BP) and that most of the Holocene was probably missing from the record.

METHODS

Field and laboratory

The AP 2007-2 core provided to us by Stephen Jackson was one of two cores he and his team recovered in October 2007. The core was collected in two successive sections each ~1 m long; coring methods are described by Liu et al. (2013). After retrieval from the field site, the AP 2007-2 core was stored at 5°C in the Laboratory of Paleoenvironmental Research at the University of Tennessee. The core was subsequently split,

https://doi.org/10.1017/qua.2016.6 Published online by Cambridge University Press

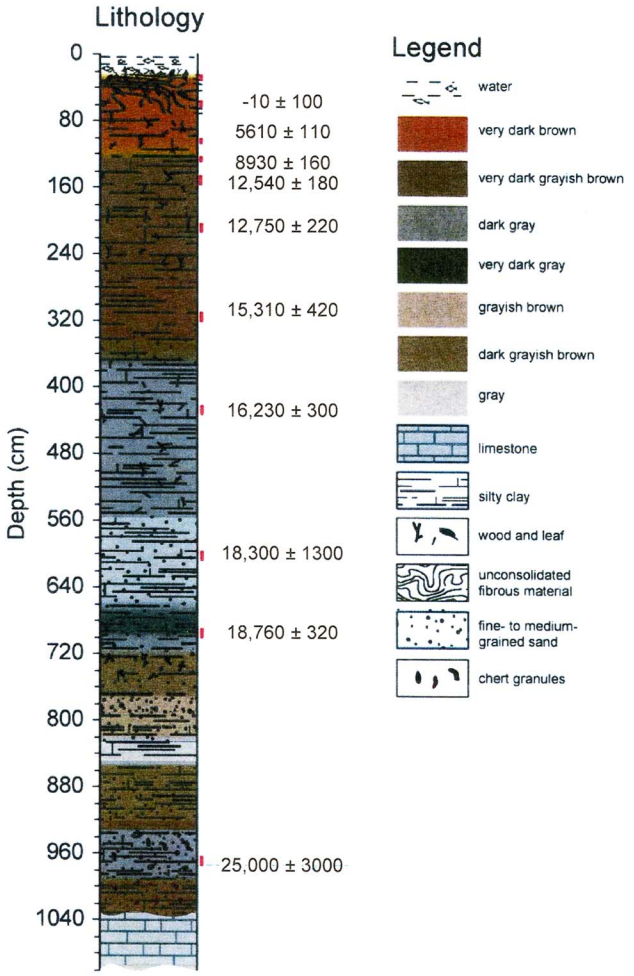

Figure 3. Original description and chronology of Anderson Pond core collected in 1976 by Hazel and Paul Delcourt, with depths reported from water surface and ages in radiocarbon years before present. Note that the late Pleistocene sedimentation rate at the site during the last glacial maximum was initially very high but was greatly reduced in the Holocene such that the upper 1.5 m of sediment has a large amount of time condensed into a thin sediment record.

and one-half was archived. One-quarter of the other half-core was sampled for thin-section preparation using a modified plastic slide box lid 3 cm wide that was pressed into the core and used to retrieve either 5 cm or 7 cm long samples, followed by air-drying for 2–3 weeks. The oriented thin-section samples were subsequently prepared by a commercial lab (Spectrum Petrographics Inc.) as either 1 × 2 cm or 5 × 7 cm thin sections. After initial scanning and digitization on a flat-bed at 600 dpi, the thin sections were examined at Baylor University using an Olympus BX51 research microscope equipped with standard plane-polarized (PPL) and crossed-polarized (XPL) light, as well as with three different wavelengths of UV fluorescence (UVf), and then photographed using a Leica digital camera. Micromorphological descriptions follow nomenclature and methods presented in Brewer (1976), Bullock et al. (1985), FitzPatrick (1993), and Stoops et al. (2010).

X-ray radiography

The split core sections of the AP 2007-2 core were examined at the University of Tennessee College of Veterinary Medicine in Knoxville, Tennessee, and imaged using standard X-ray radiography, with the hardness of the X-ray intensities adjusted to maximize contrast between the different core sediment lithologies, burrows, roots, and other organic features.

Geochronology

We submitted macrofossils from four levels of the AP 2007-2 core to the National Science Foundation Arizona AMS Laboratory and the National Ocean Sciences AMS Facility for AMS radiocarbon dating to develop a chronology for the AP 2007-2 sediment core. We also used five dates obtained by Liu et al. (2013) on the AP 2007-1 core. We adjusted the depth position of one date from the upper meter of the AP 2007-1 core to align with the stratigraphy in the AP 2007-2 core, using linear interpolation between points matched on photographs of the AP 2007-1 and 2007-2 cores (from Liu et al.'s [2013] supplementary data and others taken in our lab). We also adjusted the depth position of a macrofossil date from a crayfish burrow that had intruded older sediments, as discussed subsequently. We calibrated the radiocarbon ages and constructed an age model for the AP 2007-2 core using the program CLAM v2.2 (Blaauw, 2010) within the open-source statistical environment R v3.1.2 (R Development Core Team, 2014). We used a date of −50 ± 20 yr BP for the sediment surface, following the AP 2007-1 chronology in the Neotoma Paleoecology Database (http://www.neotomadb.org), and entered hiatuses at 65 and 95 cm based on the results of our micromorphological analysis. The CLAM age model was based on linear interpolation between dated levels, weighted by calibrated probabilities from the IntCal13 radiocarbon calibration curve (Reimer et al., 2013). The age-depth model and point estimates at increments of 1 cm were based on the weighted average of 10,000 iterations calculated by the CLAM software. We also calculated the weighted mean of the probability density distribution (Telford et al., 2004) for the calibrated ages for each date, using output from CALIB 7.02 software (Stuiver and Reimer, 1993) used with the IntCal13 data set (Reimer et al., 2013).

RESULTS

Geochronology

Table 1 shows the radiocarbon dates, calibrated age ranges, and weighted means ages of the four AMS radiocarbon dates obtained on the AP 2007-2 core and the five dates from the AP 2007-1 core (Liu et al., 2013) used in the age model. The out-of-sequence date of 6150 ± 29 cal yr BP was obtained on translocated macrofossils within a crayfish burrow that is very evident on the X-radiograph (Fig. 4). The burrow was

https://doi.org/10.1017/qua.2016.6 Published online by Cambridge University Press

Table 1. Radiocarbon dates from Anderson Pond used in the age model and calibrated age ranges.

Lab number[a]	Core[b]	Depth (cm)	Adjusted depth[c] (cm)	Material dated	$\delta^{13}C$ (‰)	^{14}C age ± 1σ (^{14}C yr BP)	Calibrated age ranges[d] 95% Confidence (cal yr BP)	Probability	Weighted mean age[e] (cal yr BP)
OS–77549	1	67	59	*Scirpus* and Polygonaceae seeds		115 ± 35	149–11	62.5	137
							175–175	0.2	
							271–186	32.2	
AA-106533	2	68	68	Seeds	−24.9	5031 ± 23	5672–5665	1.2	5807
							5774–5713	30.8	
							5797–5777	3.5	
							5893–5803	59.5	
OS-120431	2	71.5	71.5	Charcoal		5260 ± 25	6030–5936	53.9	6004
							6069–6041	6.8	
							6118–6076	22.1	
							6177–6150	1.2	
Beta–282459	2	80.5	80.5	Charcoal	−27.2	5340 ± 40	6213–5998	89.1	6148
							6268–6243	5.8	
OS–82720	1	110	110	Cyperaceae seeds		12,050 ± 60	14,065–13,757	95	13,904
OS–77548	1	118	118	*Picea* needles, Cyperaceae achene		12,050 ± 70	14,083–13,751	95	13,908
AA-106668	2	140.5	94	Uncharred plant material	−24.7	6150 ± 29	6961–6960	0.5	7063
							7159–6966	94.4	
OS–77356	1	174	174	*Picea* needle		12,550 ± 150	15,262–14,176	95	14,757
OS–79477	1	209	209	*Scirpus* achene, *Picea* seed, *Picea* needles		12,850 ± 75	15,617–15,115	95	15,350

[a]Analyses were performed by the National Ocean Sciences AMS Facility, Woods Hole Oceanographic Institute (OS); Beta Analytic (Beta); and the National Science Foundation Arizona AMS Laboratory (AA).
[b]Core 1 is the AP 2007-1 core from Anderson Pond studied by Liu et al. (2013), and dates are from that source. Core 2 is the parallel AP 2007-2 core that we studied.
[c]The depth for OS-77549 in AP 2007-1 was adjusted to the depth in AP 2007-2 by matching stratigraphy between cores. Date AA-106668 was material from a crayfish burrow that we interpret as having been brought down into the late-glacial sediments from the overlying paleosol. We use this date as a maximum age for the paleosol and position it at the bottom of the paleosol (see text).
[d]The 95% confidence intervals for the calibrated ages, and associated probabilities, are from the CLAM age model output.
[e]Weighted mean of the probability density distribution of the calibrated age, calculated from output from CALIB 7.0.2 software (Stuiver and Reimer, 1993) used with the IntCal13 data set (Reimer et al., 2013).

not visually obvious, and we selected a sample for dating from this section of the core without referring to the X-rays. The date is out of place in the second core section but provides an age estimate for paleosol sediments higher in the core, and as explained subsequently, we have used the age at a depth of 94 cm in our age model.

X-ray radiography

The X-ray radiograph shows that the upper 65 cm of the core consists of postsettlement alluvium or "legacy sediment" (James, 2013), which is well mixed by bioturbation and exhibits a sharp, erosional contact with an underlying well-dated middle Holocene (7100–5600 cal yr BP) paleosol that also shows extensive rooting (Fig. 4). A 2–3 cm diameter crayfish burrow with characteristic pelleted wall structure crosscuts organic-rich sediments and has an internal fill that appears identical to the overlying paleosol; this feature includes the "out of sequence" date based on younger macrofossils introduced by burrowing deeper into the sedimentary succession (Fig. 4). The legacy sediments interval is divisible into upper and lower subintervals, based on different opacity to X-rays, with the upper interval having a lower opacity (lighter appearance) than the lower interval. The paleosol also has a lower opacity (lighter appearance) than the underlying organic-rich sediments, which are higher opacity (darker appearance). A second unconformity corresponds to the break between the top of the lower core and the bottom of the upper core (~95 cm depth). Bioturbation is apparent through much of the core, but also with some preservation of horizontal bedding or stratification.

Scanned whole thin-section micromorphology

Representative high-resolution digital scans of whole thin sections confirm basic differences of sediment types identified on the core X-ray radiograph (Fig. 5). Legacy sediments are dark colored, have a mixed appearance, and consist of visible quartz sand and charcoal grains, as well as clasts of eroded soil material (Fig. 5A). The boundary between the top of the middle Holocene paleosol and the overlying legacy sediments is erosive and sharp, and bioturbation from the

https://doi.org/10.1017/qua.2016.6 Published online by Cambridge University Press

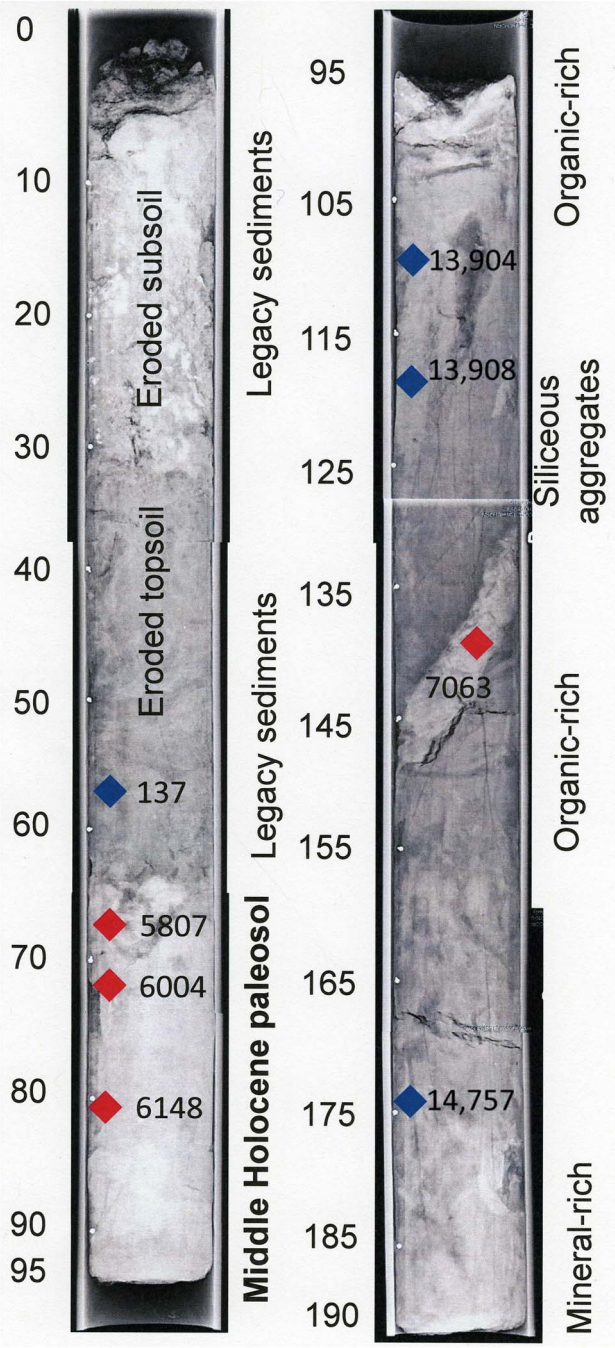

Figure 4. (color online) X-ray radiographs of the two split core sections (each 1 m long) of the AP 2007-2 core from Anderson Pond obtained by Stephen Jackson in 2007, parallel to longer core studied by Liu et al. (2013). Red diamonds show accelerator mass spectrometry (AMS) ^{14}C dates we obtained; blue diamonds are AMS ^{14}C dates obtained by Liu et al. (2013) (calibrated age ranges from Table 1). Note prominent unconformity between anthropogenic "legacy sediments" and middle Holocene paleosol, as well as prominent crayfish burrow that piped younger plant material deeper into older sediments. Location of interval with distinctive "siliceous aggregate" grains is also shown.

legacy sediments has piped darker legacy sediment material downward into the top of the paleosol, which also has abundant fine root traces (Fig. 5B). Late Pleistocene sediments are much finer grained, darker colored, and more organic rich than either the legacy sediments or the paleosol, with fine bioturbation and visible seeds and plant fragments (Fig. 5C).

Polarized light and UVf microscopy

Examples of features observed with polarized light microscopy (PPL and XPL) are shown in Figure 6, and examples of features observed with UVf microscopy are provided in Figure 7. Legacy sediments are dark colored, are well mixed by bioturbation, and contain medium to coarse sand–sized monocrystalline quartz grains along with sand-sized clasts of reworked soil material (Fig. 6A and B). In addition, these sediments have an appreciable biotic component that includes freshwater sponge spicules, charcoal grains, partially decayed plant tissues, and possibly some seeds and spores (Fig. 7A and B). The middle Holocene paleosol contains abundant fine millimeter-scale root traces, many of which are lined or coated with pedogenic clay that has a light yellow-brown color in PPL and high birefringence with bright interference colors viewed under XPL (Fig. 6C and D). Quartz silt and very fine to fine sand–sized monocrystalline quartz are abundant within the paleosol matrix, along with abundant macroscopic charcoal fragments (Fig. 6E and F). The paleosol has a biotic component that includes microscopic charcoal grains, partially decayed plant tissues, and possible seeds and spores (Fig. 7C and D). The late Pleistocene sediments are generally dark colored and very organic rich, with many organic constituents that are indistinguishable from surrounding sediment viewed with PPL but are highly visible using UVf (Fig. 7E–H). Unique types of grains occur in the core in thin-section samples prepared between 143 and 116 cm depth (location is shown in core X-ray radiograph, Fig. 4), which were termed "siliceous aggregate" grains by Ballard (2015) and Driese et al. (2015). These grains are very fine to fine sand sized and are composed of very fine to fine quartz silt grains that are cemented by a micromass of cryptocrystalline silica that has a chertlike appearance (Fig. 6G and H). Careful inspection of these grains with UVf shows some minor organic material incorporated into some of the grains; however, most are relatively pure quartz and cryptocrystalline silica.

INTERPRETATIONS AND DISCUSSION

New age-depth model

The results of micromorphological observations are summarized in Figure 8, together with a revised age-depth model based on the radiocarbon ages shown in Figure 4, but with the date obtained from translocated plant macrofossils from within a crayfish burrow used in the model as a possible age for the bottom of the paleosol by adjusting its depth to 94 cm. The upper 65 cm of the core, identified as legacy sediments, represents sediment deposited after ca. 160 cal yr BP

https://doi.org/10.1017/qua.2016.6 Published online by Cambridge University Press

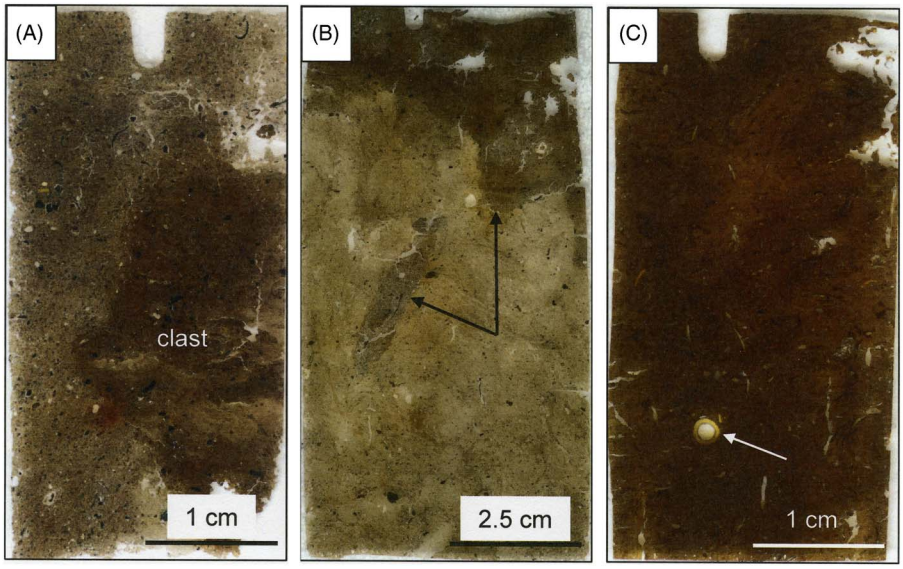

Figure 5. Scanned whole thin sections of Anderson Pond core AP 2007 sediments. (A) AP 59–63 cm depth, basal part of legacy sediment interval showing dark-colored topsoil denuded from surrounding landscape and deposited into Anderson Pond; dark flecks are charcoal, and white grains are detrital quartz. (B) AP 63–70 cm depth showing sharp boundary between dark-colored legacy sediments and middle Holocene paleosol and prominent bioturbation (arrows). (C) AP 105–109 cm depth showing top of organic-rich late Pleistocene sediments that include seed (arrow) and millimeter-scale vertical burrows or root traces (white).

(AD 1790). The lower subinterval, with a higher opacity in the X-radiograph, contains dark-colored topsoil eroded from the surrounding landscape and shows evidence of disturbance by bioturbation-related mixing. The upper subinterval, with lower opacity in the X-radiograph, appears from visual examination of the core to contain more eroded subsoil (no thin sections were prepared from this interval). Bioturbation, perhaps by crayfish, may explain the presence of traces of spruce pollen in the upper meter of the Liu et al. (2013) pollen record from Anderson Pond, in sediments deposited when spruce was rare or absent on the eastern Highland Rim. Although the crayfish burrow could have formed more recently than the paleosol, it contained charcoal and other plant macrofossils brought down from the paleosol. That the charcoal date within the burrow was both older and stratigraphically deeper than the two charcoal dates obtained from the paleosol compelled us to consider it as a possible older age limit for the paleosol. We do not know if crayfish currently inhabit Anderson Pond and if so how deep they burrow, but as a group, freshwater crayfish in North America are reported to burrow 1–9 m to reach the water table in floodplain and lake margin areas (Hasiotis et al., 2012). Modern, undetected crayfish activity could also explain the less than modern date that Liu et al. (2013) obtained at a depth of 86 cm in the AP 2007-1 core, within the paleosol layer.

The record between 160 and 5600 cal yr BP is apparently missing and was presumably removed either by erosion preceding emplacement of the overlying legacy sediments or by widespread oxidation of wetland sediments during subaerial exposure (Fig. 8). The interval from 95 to 65 cm depth represents middle Holocene soil formation with 30 cm sediment accumulation over a period from 7100 to 5600 cal yr BP. There is no early Holocene date from the core, and we attribute this to the existence of a second unconformity resulting from either erosion prior to deposition of the middle Holocene paleosol sediments or widespread oxidation of wetland sediments during subaerial exposure. The Pleistocene–Holocene boundary at 11,600 cal yr BP is within the modeled hiatus (Fig. 8). Based on our new age-depth model, the occurrences of siliceous aggregate grains from 143 to 116 cm depth correspond to the period from 14,300 to 13,900 cal yr BP. Ballard (2015) interpreted siliceous aggregate grains as originating during intense fires that generated large amounts of completely combusted wood ash (with little or no charcoal), which raised the pH sufficiently to solubilize biogenic, opaline silica that was then available to cement loessial quartz silt to form siliceous aggregate grains. Her hypothesis for siliceous aggregate grain formation was based on archaeological studies by Weiner (2010), who had previously postulated that siliceous aggregates associated with hearth surfaces are indicators of fire; this hypothesis was subsequently verified through laboratory experiments described in Ballard (2015).

Applying our new age model and micromorphological interpretations to the Anderson Pond pollen and charcoal records

In Figure 9, we apply our new age model for the upper section of the Anderson Pond profile to previous pollen and charcoal analyses. All data are plotted by depth extrapolated to the AP 2007-2 core, together with interpolated ages. Pollen data

https://doi.org/10.1017/qua.2016.6 Published online by Cambridge University Press

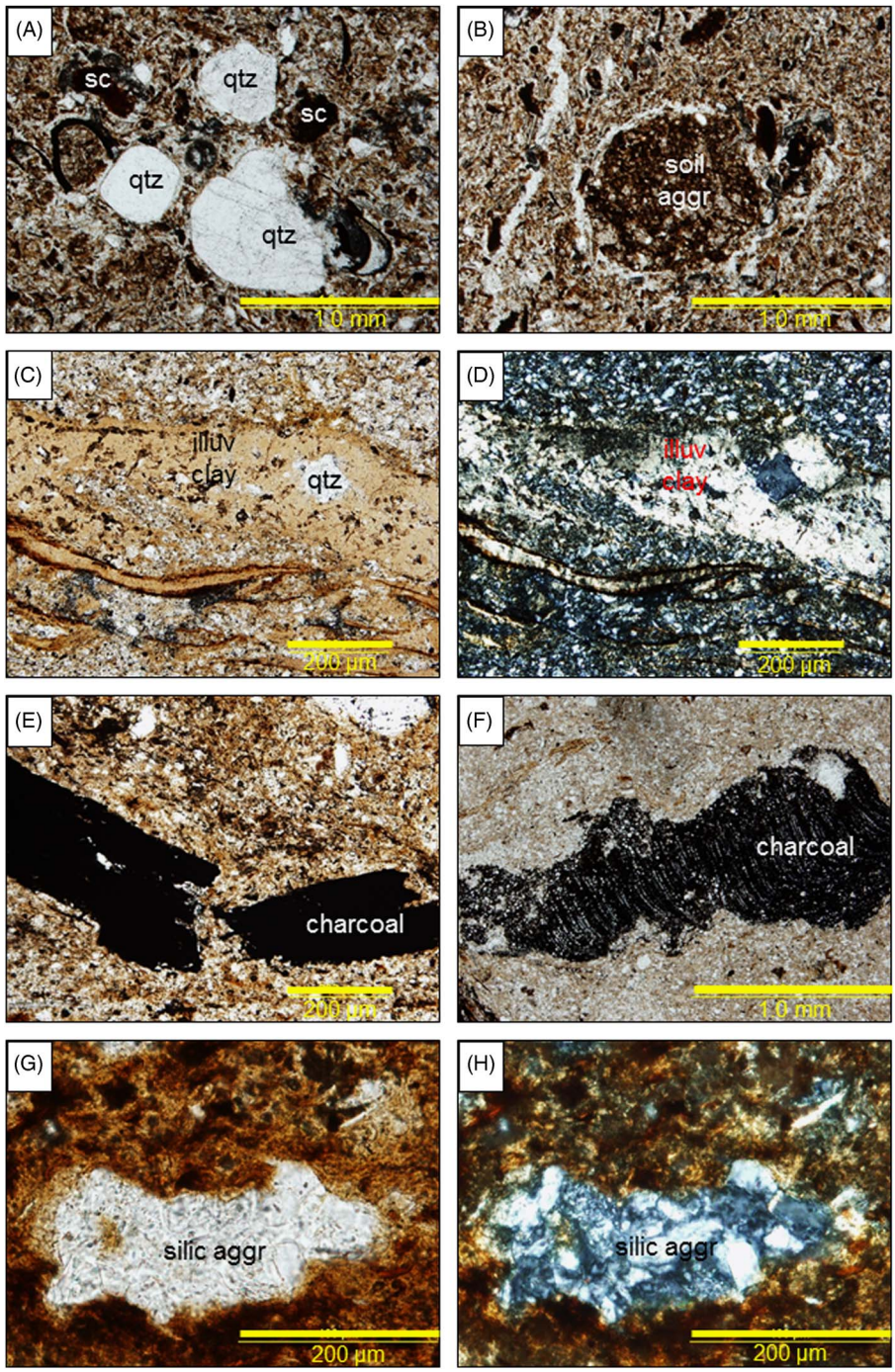

Figure 6. Anderson Pond thin-section micrographs from sediment cores. (A) AP 48–52 cm depth, medium to coarse sand–sized quartz grains (qtz) and soil clasts (sc) transported by high-energy flows, lower part of legacy sediments (plane-polarized light [PPL]). (B) AP 48–52 cm depth, reworked dark soil aggregates (soil aggr) denuded from surrounding landscape and deposited into Anderson Pond (PPL). (C, D: PPL and cross-polarized light [XPL]) AP 71–74 cm depth, root channels in middle Holocene paleosol filled with yellowish illuviated clay (illuv clay) under PPL, exhibiting bright interference colors and flecked extinction pattern under XPL. (E) AP 76–82 cm depth, macroscopic charcoal grain that is broken (PPL). (F) AP 83–87 cm depth, large macroscopic charcoal grain with relict plant cell structure preserved. (G, H: PPL and XPL) AP 116–119 cm depth showing typical example of siliceous aggregate (silic aggr) grain composed of fine to very fine silt–sized loessial quartz grains cemented by cryptocrystalline silica.

from the recent study by Liu et al. (2013) of the parallel AP 2007-1 core were downloaded from the Neotoma Paleoecology Database (http://www.neotomadb.org). Depths in the first section of the AP 2007-1 core were adjusted to depths in the AP 2007-2 core using linear interpolation between five match points based on stratigraphy. Depths in the second core

https://doi.org/10.1017/qua.2016.6 Published online by Cambridge University Press

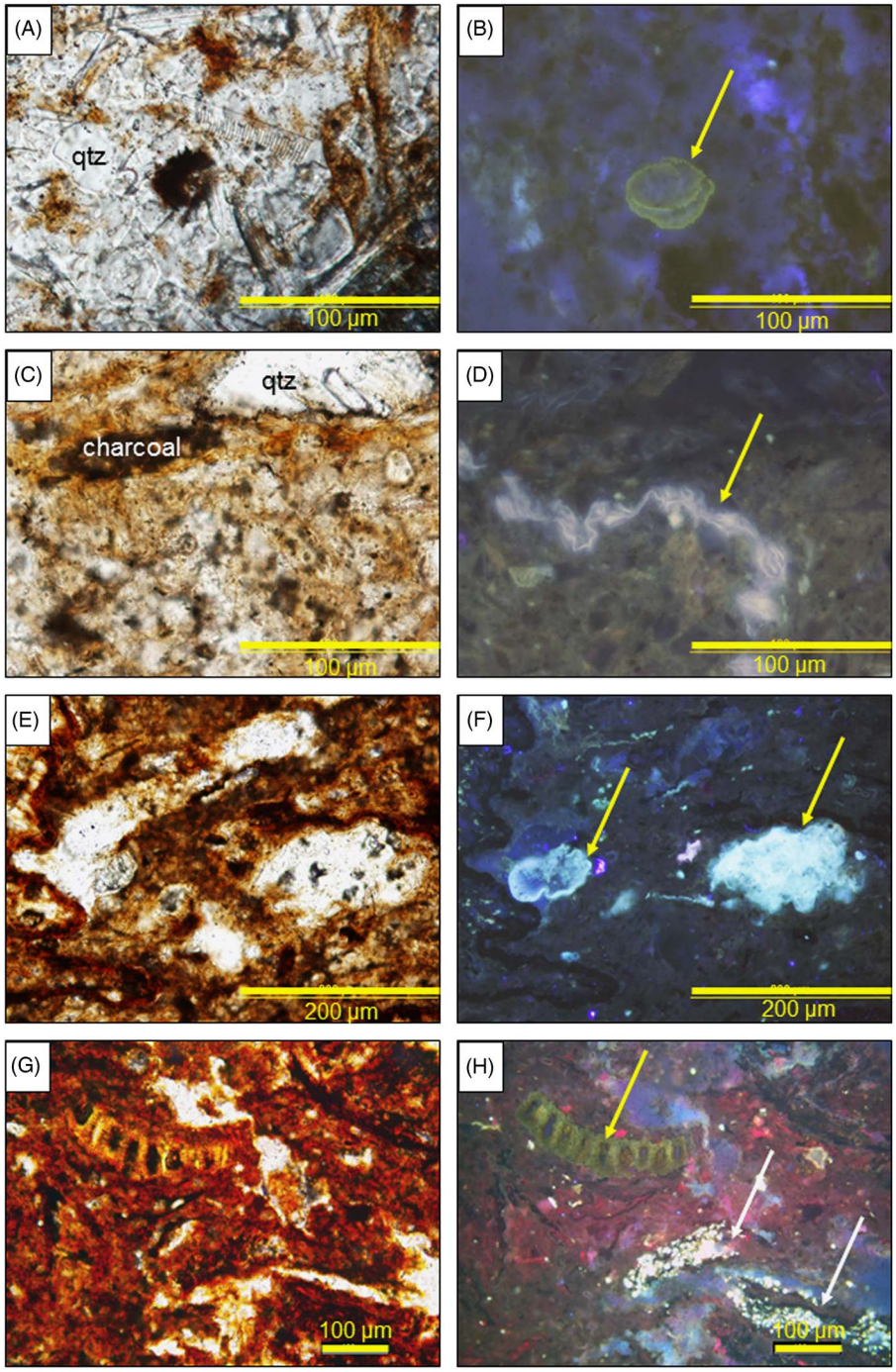

Figure 7. Anderson Pond thin-section micrographs from sediment cores. All photos are paired plane-polarized light [PPL] and UV fluorescence (UVf). (A, B) AP 48–52 cm depth, legacy sediment rich in quartz (qtz) and freshwater sponge spicules (elongate, clear grains in PPL) and containing organic grain (spore?) visible only under UVf (yellow arrow). (C, D) AP 88–94 cm depth, quartz (qtz) and charcoal-rich sediment of middle Holocene paleosol containing fine organic matter visible only under UVf (yellow arrow). (E, F) AP 116–119 cm depth, organic-rich sediment containing clumps of organic material of uncertain affinity, visible only under UVf (yellow arrows). (G, H) AP 126–129 cm depth, organic-rich sediment containing fragment of stem or root of aquatic plant (yellow arrow) as well as minute fluorescent white spherules (white arrows) visible only under UVf.

section were not adjusted. Pollen data for the core recovered by Delcourt in 1976 were taken from the Neotoma Paleoecology Database and from Delcourt (1978); microscopic charcoal data are from Ballard et al. (2016). We matched these proxies from the AP 1976 core to depths in the AP 2007-2 core using loss-on-ignition data from Delcourt (1978), assuming that the interval of low organic content from 124 to 88 cm in the AP 1976 core (depths measured

https://doi.org/10.1017/qua.2016.6 Published online by Cambridge University Press

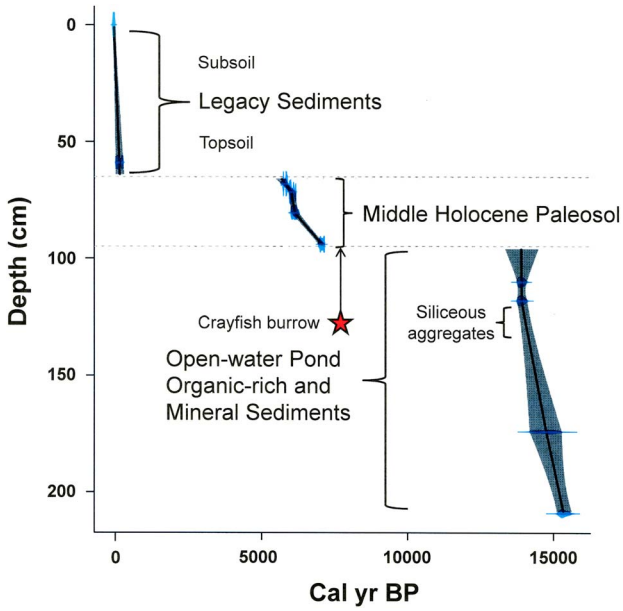

Figure 8. (color online) Summary showing interpreted age model for 2 m long AP 2007-2 core, annotated with occurrences of important micromorphological features. Note that legacy sediments unconformably overlie a middle Holocene paleosol that contains illuviated clay and charcoal and which was characterized by greatly reduced sediment accumulation rates. Note also that siliceous aggregate grains occur in a narrow time interval, in association with organic-rich sediment.

from water surface) corresponded to the paleosol. We positioned the sediment–water interface of the 1976 profile (25 cm) at 8 cm in the AP 2007-2 core based on our age model and used these match points and the top and bottom of the paleosol to linearly adjust depths in the legacy sediments and paleosol. For depths below the paleosol in the AP 1976 core, we subtracted 29 cm, the offset between the bottom of the paleosol in the AP 1976 core (124 cm) and in the AP 2007-1 profile (95 cm).

The new age model and micromorphological analyses, as summarized in Figure 9, confirm some previous interpretations of the Anderson Pond sediment record and lead to reevaluation of others. Our results support the interpretation of Liu et al. (2013) that the Anderson Pond record contains one or more depositional hiatuses during the late-glacial period and Holocene. The profile is not a record of continuous sedimentation, as advanced by Delcourt (1979) and Delcourt and Delcourt (1980), but instead contains sediments associated with three distinct intervals of sediment deposition separated by two prolonged hiatuses: late-glacial sediments that extend to ca. 13,900 cal yr BP, a mid-Holocene interval from 7100 to 5600 cal yr BP reflecting processes operating under subaerial conditions, and legacy sediments deposited since ca. AD 1790 with lower (topsoil) and upper (subsoil) subintervals (Fig. 9).

The interval of low fire activity that Ballard et al. (2016) identified in the AP 1976 core, coincident with high pollen percentages for fire-intolerant taxa such as *Ostrya*, predates rather than spans the early Holocene, which is apparently missing from the AP 1976 core and the cores collected in 2007 (Liu et al., 2013), based on our core matchup. The period of low fire activity and mixed mesophytic vegetation falls entirely within the late-glacial sediments and is truncated by the hiatus below the paleosol. However, our micromorphological analyses and new mid-Holocene AMS dates confirm the interpretation of Ballard et al. (2016) that the interval of high charcoal concentrations in the AP 1976 core corresponds to an interval of drier climate during the middle Holocene, which led to increased fires at Anderson Pond, in areas surrounding the sinkhole and at some times in the interior. Delcourt (1979) had interpreted shifts in pollen and plant macrofossil assemblages and influx to indicate a lowering of water level and expansion of swamp shrubs including *Alnus* and *Cephalanthus* in the interior of Anderson Pond associated with a warming and drying climate during the hypsithermal interval. In a later article, Delcourt and Delcourt (1980) tied the higher percentages of indeterminate pollen in this part of the core (Figure 9) to increased oxidation and possibly increased microbial activity at this time of lower water level, which damaged high numbers of pollen grains to the extent that taxonomic identification was not possible.

The paleosol root pores lined with illuviated clay visible on thin sections from the AP 2007-2 core confirm these previous interpretations of lower water level and increased oxidation of sediments during the middle Holocene. The paleosol also shows mineral weathering, and no signs of redoximorphy associated with saturated soils, indicating sustained periods of well-drained conditions at the core site. Below that, separated by a hiatus, core sediments reflect deposition in a late-glacial pond. We concur with the original interpretation of Delcourt (1979) that *Alnus* and other shrubs established in Anderson Pond in association with postglacial climate and environmental changes that converted the pond to a swamp. However, the sediments that correspond to this conversion, in which we would expect pollen evidence of the initial arrival and spread of *Alnus* in the pond interior, are missing from the record, part of the hiatus in the latest Pleistocene and early Holocene. Although *Alnus* is typically associated with wet conditions, the species that presently grows at Anderson Pond, *Alnus serrulata*, can grow in well-drained upland soils and under saturated conditions (US Department of Agriculture, Natural Resources Conservation Service, 2016). Thus, some *Alnus* shrubs may have persisted during middle Holocene conditions of unsaturated soils in the sinkhole, when the paleosol formed. It is also possible that small areas of ponded drainage existed in the interior of Anderson Pond, other than at the core site, during the middle Holocene, and that *Alnus* shrubs grew in those locations. *Alnus* is wind pollinated, and the pollen in the paleosol also could have come from plants growing on the rim of the sinkhole or in surrounding upland areas.

Our interpretation that the upper 65 cm of the 2007-2 core consists of legacy sediments puts the settlement horizon

https://doi.org/10.1017/qua.2016.6 Published online by Cambridge University Press

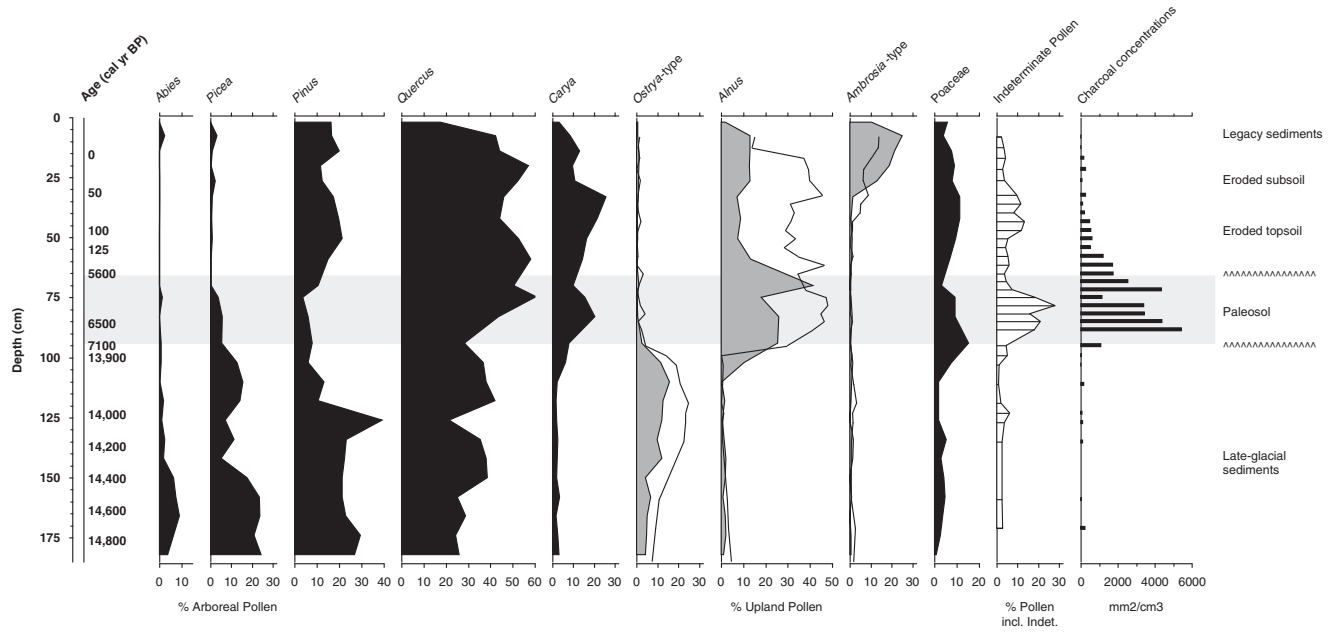

Figure 9. Pollen percentages and charcoal concentrations in the upper 1.8 m of the Anderson Pond record, showing ages based on our new model informed by micromorphological analysis. Data are plotted by depths extrapolated to the AP 2007-2 core, with two hiatuses and the intervals of late-glacial sediments, paleosol, and legacy sediments demarcated based on thin-section analysis and radiocarbon dating. Pollen percentages shown as curves shaded black or gray are from analyses of the AP 2007-1 core by Liu et al. (2013). Unshaded, overlain curves and indeterminate pollen percentages are from analyses of the AP 1976 core by Delcourt (1978, 1979). Pollen sums follow Delcourt (1979). Charcoal concentration data are from Ballard et al. (2016), based on analyses of the original pollen slides from the AP 1976 core.

~20–40 cm below the rise in *Ambrosia* pollen in the pollen records of Delcourt (1979) and Liu et al. (2013), as indicated in Figure 9. Increased percentages of *Ambrosia* pollen are widely used as an indicator of Euro-American settlement in pollen studies in eastern North America (McAndrews, 1988), with the position of the "*Ambrosia* rise" often used in age models (e.g., Booth et al., 2016). Delcourt (1979) stated that Euro-American land clearance, settlement, and cultivation began in the late 1700s on the Highland Rim of Tennessee, and she interpreted the lowest occurrence of *Ambrosia* pollen to mark initial land clearance and settlement around Anderson Pond at ca. AD 1790. The CLAM age modeling produced a point estimate for the bottom of the legacy sediment of 156 cal yr BP (AD 1794), which corresponds well with this land-use history. However, the position of the *Ambrosia* rise within the legacy sediment interval is inconsistent with the expected correlation between postsettlement alluvium and *Ambrosia* pollen. That *Ambrosia* pollen is negligible or rare in the lower subinterval of legacy sediment interpreted to reflect topsoil washed into the basin may indicate that this agricultural weed did not establish with initial forest clearance and agricultural development. The delay could indicate that the plant only became important surrounding Anderson Pond in a later stage of Euro-American activity, when fields were more deeply eroded and sediment derived from more clay-rich subsoils began to be deposited in the sinkhole. Our finding, based on thin-section analysis, that peak *Ambrosia* percentages at Anderson Pond do not indicate the settlement horizon but instead postdate it leads us to wonder whether such a delay might be present in other records for which the pollen type has been use as a stratigraphic marker.

Comparisons with correlative floodplain, wetland, and speleothem records

Our interpretation of the development of a middle Holocene paleosol at Anderson Pond adds to other evidence suggesting dry mid-Holocene conditions in Tennessee and elsewhere in the eastern and central United States. Previous research by Driese et al. (2008) on a small floodplain just north of Chattanooga, Tennessee, established evidence for four repeated episodes of middle Holocene drought, each estimated to be between 200 and 400 yr duration, based on 2–5 per mil excursions in the $\delta^{13}C$ values of soil organic matter (SOM) preserved in floodplain soils and paleosols. Kocis (2011) obtained similar results from study of $\delta^{13}C$ values of SOM obtained from Tennessee River floodplain sites in eastern Tennessee and northeastern Alabama, which also showed evidence for episodic drought conditions during the middle Holocene.

Crownover et al. (1994) excavated sediments of an upland doline in Oak Ridge, Tennessee, and found two paleosols. Soil humates from the upper paleosol, which was overlain by sediments associated with postsettlement agriculture, yielded

https://doi.org/10.1017/qua.2016.6 Published online by Cambridge University Press

a radiocarbon date of 320 ± 70 ^{14}C yr BP, whereas a humate date for the lower paleosol showed it to be of mid-Holocene age (6100 ± 100, 95% confidence range of 7244–6741 cal yr BP). No micromorphological or microfossil analyses were available for the site, but based on pedogenic characteristics of the paleosol and the lack of evidence of pedogenesis in the underlying sediments, the authors interpreted the mid-Holocene paleosol to indicate a period of warming and drying climate associated with the hypsithermal. A recent study by Tanner et al. (2015) of a bog in southwestern North Carolina also presented sedimentary proxy evidence of a mid-Holocene "hypsithermal event" characterized by less negative δ^{13}C values of SOM and by organic biomarker n-alkane distributions that show an increase of the C_{18} chain length during the middle Holocene; C_{18} is a biomarker for bacteria and suggests organic matter breakdown, which would be expected in a warm, dry climate with extensive organic matter oxidation. Comparison with Holocene records from the US Great Plains (Nordt et al., 2008) and the middle Atlantic region of the United States (Stinchcomb et al., 2013) indicates that the stable carbon isotope expression of the middle Holocene thermal maximum shows evidence for at least two, and possibly as many as four, major episodes of drought in the Great Plains and middle Atlantic regions, manifested by excursions of 2–5 per mil toward less negative δ^{13}C values. However, a major problem with these soil- and paleosol-based proxies is that they have poorer geochronological control (e.g., many are based on AMS ^{14}C dating of bulk SOM) and thus can only be considered as providing coarse-scale paleoclimate resolution.

A recent study by Driese et al. (2016a) analyzed annual speleothem layers in a stalagmite (RM0710-2-1) obtained from Raccoon Mountain Cave near Chattanooga, Tennessee, spanning the entire middle and late Holocene (from 7600 yr BP to ca. 400 yr BP), and applied rigorous time series models to a very high-resolution data set of 4796 annual UVf layers observed in thin sections. The middle Holocene paleoclimate record was interpreted as characterized by 100–400 yr intervals dominated by wetter conditions with thinner UVf layers with more negative δ^{13}C values, punctuated by abrupt onset of shorter periods (5–50 yr, rarely 100 yr) of lower rainfall with thicker UVf deposits with less negative δ^{13}C values; short-duration (<5 yr) low-rainfall "extreme drought" events had very thick annual deposits and the least negative δ^{13}C values. The late Holocene, in comparison, was characterized by overall wetter conditions and more regular (sinusoidal curve) behavior suggesting 50–100 yr cycles of higher and lower rainfall, with overall thinner UVf layers than observed in the middle Holocene portion of the speleothem. The thin early Holocene speleothem record had multiple erosion/dissolution surfaces with common terra rossa sediment drapes, interpreted as evidence that cave water levels were high during the latest Pleistocene and early Holocene such that the stalagmite was submerged by cave streams and cave sediments and growth was interrupted (Driese et al., 2016a).

CONCLUSIONS

1. Although the sediment record at Anderson Pond, eastern Tennessee, spans the late Pleistocene to Holocene, from ca. 25,000 cal yr BP to the present, the late-glacial period and Holocene (<13,900 cal yr BP) are incomplete because of oxidation and soil formation. Whereas the three subintervals recognized in the upper 1.85 m of the profile include sediments that range in age from ca. 14,850 to –50 cal yr BP, two hiatuses account for more than 12,000 missing years of sediment record in this sequence.
2. Both X-ray radiography and thin-section micromorphology reveal that the upper 65 cm of the AP 2007-2 core comprises "legacy sediments" that record anthropogenic disturbance <160 cal yr BP.
3. An unconformity separates legacy sediments from a subjacent paleosol (95–65 cm depth) that has root traces, illuviated clay, and charcoal fragments, and which formed between 7100 and 5600 cal yr BP; during this period of warm, dry conditions characterizing the middle Holocene thermal maximum. At this time, Anderson Pond became desiccated, subaerially exposed, and converted to a vegetated soil system, and associated wetland sediments were highly oxidized.
4. A second major unconformity indicates a hiatus associated with either early Holocene erosion or oxidation of wetland sediments during subaerial exposure, and, as a consequence, the middle Holocene paleosol is juxtaposed directly on top of the late Pleistocene organic-rich sediments.
5. Siliceous aggregate grains occur within the depth interval of 143–116 cm, corresponding to 14,300–13,900 cal yr BP and indicating the occurrence of intense fires.

Although thin sections are not commonly used in studies of paleoclimate from Quaternary lacustrine sediments, we hope that our study is an example that will encourage greater use of micromorphology in multianalytical approaches because it greatly enhances resolution of depositional and pedogenic processes.

ACKNOWLEDGMENTS

The authors gratefully acknowledge support of National Science Foundation (NSF) EAR-0823131 awarded to SGD and EAR-0822824 awarded to SPH and ZL for this research on late Pleistocene–Holocene paleoclimate reconstruction in the southern Appalachian region. Additional support was provided by the Baylor University Department of Geosciences and the University of Tennessee Department of Geography. We thank Stephen Jackson for providing the core we analyzed (collected with funding from NSF DEB-0716951) and Jim Kocis for assistance in the field and lab. We also acknowledge the data contributors and the Neotoma community (Neotoma Paleoecology Database, http://www.neotomadb.org). We gratefully acknowledge input from *Quaternary Research* Associate Editor Robert Booth and reviewers B. Tanner and D. Peteet that improved the manuscript.

REFERENCES

Ballard, J.P., 2015. Evidence of Late Quaternary Fires from Charcoal and Siliceous Aggregates in Lake Sediments in the Eastern U.S.A. PhD dissertation, University of Tennessee, Knoxville.

Ballard, J.P., Horn, S.P., Li, Z.-H., 2016. A 23,000-year microscopic charcoal record from. Anderson Pond, Tennessee, USA. Palynology (in press). http://dx.doi.org/10.1080/01916122.2016.1156588.

Blaauw, M., 2010. Methods and code for 'classical' age-modelling of radiocarbon sequences. *Quaternary Geochronology* 5, 512–518.

Blaauw, M., Christen, J.A., 2011. Flexible paleoclimate age-depth models using an autoregressive gamma process. *Bayesian Analysis* 6, 457–474.

Booth, R.K., Ireland, A.W., LeBouf, K., Hesel, A., 2016. Late Holocene climate-induced forest transformation and peatland establishment in the central Appalachians. *Quaternary Research* 85, 204–210.

Brauer, A., 2004. Annually laminated lake sediments and their palaeoclimatic relevance. In: Sischer, H., Kumke, T., Lohmann, G., Flöser, G., Miller, H., Storch, H., von Negendank, J.F.W. (Eds.), The Climate in Historical Times. Springer, Berlin, pp. 111–128.

Brewer, R., 1976. Fabric and Mineral Analysis of Soils. 2nd ed. Robert E. Krieger, Huntington, New York.

Bullock, P., Fédoroff, N., Jungerius, A., Stoops, G., Tursina, T., Babel, U., 1985. Handbook for Soil Thin Section Description. Waine Research, Wolverhampton, UK.

Clark, J.S., 1988. Stratigraphic charcoal analysis on petrographic thin sections: application to fire history in northwestern Minnesota. *Quaternary Research* 30, 81–91.

Crownover, S.H., Collins, M.E., Lietzke, D.A., 1994. Soil-stratigraphic correlation of a doline in the Ridge and Valley province. *Soil Science of America Journal* 58, 1730–1738.

Delcourt, H.R., 1978. Late Quaternary Vegetation History of the Eastern Highland Rim and Adjacent Cumberland Plateau of Tennessee. PhD dissertation, University of Minnesota, Minneapolis.

Delcourt, H.R., 1979. Late Quaternary vegetation history of the eastern Highland Rim and adjacent Cumberland Plateau of Tennessee. *Ecological Monographs* 49, 255–280.

Delcourt, P.A., Delcourt, H.R., 1980. Pollen preservation and Quaternary environmental history in the southeastern United States. *Palynology* 4, 215–231.

Driese, S.G., Ashley, G.M., 2016. Paleoenvironmental reconstruction of a paleosol catena, the Zinj archaeological level, Olduvai Gorge, Tanzania. *Quaternary Research* 85(1), 133–146.

Driese, S.G., Horn, S.P., Ballard, J.P., Li, Z.-H., Boehm, M.S., 2015. Micromorphological interpretation of late Pleistocene to Holocene paleoenvironmental history of Anderson Pond, Tennessee, USA. *Geological Society of America, Abstracts with Programs* 47(7), 129.

Driese, S.G., Li, Z.-H., Cheng, H., Harvill, J.L., Sims, J., 2016a. High-resolution rainfall records for middle and late Holocene based on speleothem annual UV fluorescent layers integrated with stable isotopes and U/Th dating, Raccoon Mountain Cave, TN, USA. In: Feinberg, J., Gao, Y., Alexander, E.C., Jr. (Eds.), *Caves and Karst across Time. Geological Society of America, Special Papers 516*. Geological Society of America, Boulder, CO, pp. 231–246.

Driese, S.G., Li, Z.-H., McKay, L.D., 2008. Evidence for multiple, episodic, mid-Holocene Hypsithermal recorded in two soil profiles along an alluvial floodplain catena, southeastern Tennessee, USA. *Quaternary Research* 69, 276–291.

Driese, S.G., Orvis, K.H., Horn, S.P., Li, Z.-H., Jennings, D.S., 2007. Paleosol evidence for Quaternary uplift and for climate and ecosystem changes in the Cordillera de Talamanca, Costa Rica. *Palaeogeography, Palaeoclimatology, Palaeoecology* 248, 1–23.

Driese, S.G., Peppe, D.J., Beverly, E.J., DiPietro, L.M., Arellano, L.N., Lehmann, T., 2016b. Paleosols and paleoenvironments of the early Miocene deposits near Karungu, Lake Victoria, Kenya. *Palaeogeography, Palaeoclimatology, Palaeoecology* 443, 167–182.

FitzPatrick, E.A., 1993. *Soil Microscopy and Micromorphology*. John Wiley and Sons, New York.

Hasiotis, S.T., Platt, B.F., Reilly, M., Amos, K., Lang, S., Kennedy, D., Todd, J.A., Michel, E., 2012. Actualistic studies of the spatial and temporal distribution of terrestrial and aquatic organism traces in continental environments to differentiate lacustrine from fluvial, eolian, and marine deposits in the geological record. In: Baganz, O.W., Bartov, Y., Bohacs, K., Nummedal, D. (Eds.), *Lacustrine Sandstone Reservoirs and Hydrocarbon Systems. American Association of Petroleum Geologists (AAPG) Memoir 95*. AAPG, Tulsa, OK, pp. 433–489.

James, L.A., 2013. Legacy sediment: definition and processes of episodically produced anthropogenic sediment. *Anthropocene* 2, 16–26.

Kocis, J.J., 2011). Late Pleistocene and Holocene Hydroclimate Change in the Southeastern United States: Sedimentary, Pedogenic, and Stable Carbon Isotope Evidence in Tennessee River Floodplain Paleosols. Master's thesis, University of Tennessee, Knoxville.

Liu, Y., Andersen, J.J., Williams, J.W., Jackson, S.T., 2013. Vegetation history in central Kentucky and Tennessee (USA) during the last glacial and deglacial periods. *Quaternary Research* 79, 189–198.

McAndrews, J.H., 1988. Human disturbance of North America forests and grasslands: the fossil pollen record. In: Huntley, B., Webb, T., III (Eds.), *Vegetation History*. Kluwer, Dordrecht, the Netherlands.

Nordt, L., Von Fisher, J., Tieszen, L., Tubbs, J., 2008. Coherent changes in relative C4 plant productivity and climate during the late Quaternary in the North American Great Plains. *Quaternary Science Reviews* 27, 1600–1611.

R Development Core Team. 2014. *R: A Language and Environment for Statistical Computing*. R Foundation for Statistical Computing, Vienna.

Reimer, P.J., Bard, E., Bayliss, A., Beck, J.W., Blackwell, P.G., Ramsey, C.B., Buck, C.E., et al., 2013. IntCal13 and Marine13 radiocarbon age calibration curves 0–50,000 years cal BP. *Radiocarbon* 55(4), 1869–1887.

Stinchcomb, G.E., Messner, T.C., Williamson, F.C., Driese, S.G., Nordt, L.C., 2013. Climatic and human controls on Holocene floodplain vegetation changes in eastern Pennsylvania based on the isotopic composition of soil organic matter. *Quaternary Research* 79, 377–390.

Stoops, G., Marcelino, V., Mees, F. (Eds.), 2010. *Interpretation of Micromorphological Features of Soils and Regoliths*. Elsevier, Amsterdam.

Stuiver, M., Reimer, P.J., 1993. Extended ^{14}C data base and revised CALIB 3.0 ^{14}C age calibration program. *Radiocarbon* 35(1), 215–230.

Tanner, B.R., Lane, C.S., Martin, E.M., Young, R., Collins, B., 2015. Sedimentary proxy evidence of a mid-Holocene hypsithermal event in the location of a current warming hole, North Carolina, USA. *Quaternary Research* 83, 315–323.

Telford, R.J., Heegaard, E., Birks, H.J.B., 2004. The intercept is a poor estimate of calibrated radiocarbon age. *Holocene* 14, 296–298.

US Department of Agriculture, Natural Resources Conservation Service. 2016. PLANTS Database (accessed October 25, 2016). http://plants.usda.gov.

van der Meer, J.J.M., Menzies, J., 2011. The micromorphology of unconsolidated sediments. *Sedimentary Geology* 238, 213–232.

Weiner, S., 2010. *Microarchaeology: Beyond the Visible Archaeological Record*. Cambridge University Press, New York.

https://doi.org/10.1017/qua.2016.6 Published online by Cambridge University Press